processes

MDPI

Article

Cooling and Water Production in a Hybrid Desiccant M-Cycle Evaporative Cooling System with HDH Desalination: A Comparison of Operational Modes

Lanbo Lai [1], Xiaolin Wang [1,*], Gholamreza Kefayati [1] and Eric Hu [2]

[1] School of Engineering, University of Tasmania, Hobart, TAS 7001, Australia
[2] School of Mechanical Engineering, the University of Adelaide, Adelaide, SA 5005, Australia
* Correspondence: xiaolin.wang@utas.edu.au

Highlights:

What are the main findings?

- A hybrid desiccant M-cycle cooling system with an HDH unit is proposed for simultaneous cooling and water production.
- Three typical operational modes are analysed and compared in terms of cooling and water production.

What is the implication of the main finding?

- The recirculation mode exhibited a superior cooling performance than the other two modes.
- The water production rates and system COP were similar among the three modes.

Abstract: In this paper, the cooling and freshwater generation performance of a novel hybrid configuration of a solid desiccant-based M-cycle cooling system (SDM) combined with a humidification–dehumidification (HDH) desalination unit is analysed and compared in three operational modes: ventilation, recirculation, and half recirculation. The HDH unit in this system recycles the moist waste air sourced from the M-cycle cooler and rotary desiccant wheel of the SDM system to enhance water production. A mathematical model was established and solved using TRNSYS and EES software. The results of this study indicate that the recirculation mode exhibited superior cooling performance compared to the other two modes, producing up to 7.91 kW of cooling load and maintaining a supply air temperature below 20.85 °C and humidity of 12.72 g/kg under various ambient conditions. All the operational modes showed similar water production rates of around 52.74 kg/h, 52.43 kg/h, and 52.14 kg/h for the recirculation, half-recirculation and ventilation modes, respectively, across a range of operating temperatures. The recirculation mode also exhibited a higher COP compared to the other modes, as the environmental temperature and relative humidity were above 35 °C and 50%. However, it should be noted that the implementation of the recirculation mode resulted in a higher water consumption rate, with a maximum value of 5.52 kg/h when the inlet air reached 45 °C, which partially offset the benefits of this mode.

Keywords: M-cycle; evaporative cooling; solid desiccant; humidification–dehumidification desalination; water production

Citation: Lai, L.; Wang, X.; Kefayati, G.; Hu, E. Cooling and Water Production in a Hybrid Desiccant M-Cycle Evaporative Cooling System with HDH Desalination: A Comparison of Operational Modes. *Processes* **2023**, *11*, 611. https://doi.org/10.3390/pr11020611

Academic Editors: Yabin Guo, Zhanwei Wang, Yunpeng Hu and João M. M. Gomes

Received: 26 January 2023
Revised: 14 February 2023
Accepted: 15 February 2023
Published: 16 February 2023

1. Introduction

The increasing demand for thermal comfort and water, driven by economic development and population expansion, has created significant challenges related to energy and water efficiency for sustainable development [1]. The International Energy Agency (IEA) has reported that 10% of global electricity is used for cooling, which contributes to 10% of global greenhouse gas emissions. This value is expected to be tripled by 2050 [2].

In addition, freshwater is becoming a scarce resource as more countries are facing water stress [3]. Currently, around 20% of the world's population lives in areas with water scarcity, and the situation is expected to worsen, with up to 40% of the global population facing water shortage by 2030 [4].

Indirect evaporative cooling (IEC) has gained increasing research interest due to its energy efficiency and environmentally friendly features, making it a potential replacement for mechanical vapour compression systems [5]. The IEC can significantly reduce the supplied air temperature to approximate the ambient wet-bulb temperature (WBT) without augmenting the moisture content [6]. This technology eliminates the need for chemical refrigerants and mechanical compressors, as the cooling process is completed by water evaporation [7]. In 2002, a novel thermodynamic cycle of IEC was developed by Maisotsenko, also known as the M-cycle [8]. In this cycle, a fraction of the pre-cooled supply air is redirected to wet channels as the working air, allowing the product air to be cooled below the WBT and towards the dew point temperature (DPT) of the incoming air at a constant humidity level [9,10]. However, the M-cycle's performance is greatly influenced by the ambient relative humidity. The literature suggests that the M-cycle is most effective when the ambient relative humidity is below 70% [11,12]. Hybridising the M-cycle cooler and a solid desiccant wheel is often regarded as an effective approach to improve the M-cycle cooler's performance in humid environments [12,13].

Goldsworthy and White [14] optimised a solid desiccant evaporative cooling system by changing the secondary/primary ratio of the IEC and the process-to-regeneration ratio of the desiccant wheel. The results showed that the highest COP could reach more than 20, while the secondary/primary ratio of the IEC was 0.67, and the process-to-regeneration ratio of the desiccant wheel was 0.3. Gao et al. [15] numerically evaluated a solid desiccant-based IEC cooling system. It was found that the optimum inlet air humidity ratio and temperature should be no more than 18 g/kg and 35 °C, respectively. Three novel two-stage desiccant cooling systems integrated with the Maisotsenko cooling cycle were developed and analysed by Gadalla and Saghafifar [16]. They concluded that the two-stage Maisotsenko desiccant system with inlet air pre-cooling was effective in minimising the energy usage of air conditioning systems in humid environments. This system was recommended for use in buildings during peak times. Lin et al. [17] examined the impact of removing humidity from the inlet air on the M-cycle cooler's cooling performance. Their results indicated a 70–135% cooling performance and energy efficiency increment after introducing a dehumidification process for the M-cycle. Kashif Shahzad et al. [18] conducted the first experimental work on integrating a solid dehumidification system with an M-cycle cooler (cross-flow type). The proposed system was tested and assessed with a traditional solid desiccant-based cooling system under various inlet air parameters. It was observed that the investigated system was 60% to 65% more efficient in thermal COP than the conventional system. Pandelidis et al. [19] presented four novel desiccant cooling systems based on pre-cooling the inlet air with different M-cycle IECs. It was found the most efficient configuration consisted of a cross-flow M-cycle as a pre-cooler and a regenerative M-cycle as a post-cooler. Delfani and Karami [20] performed research on solar-powered desiccant M-cycle IEC systems using TRNSYS software. They proposed three novel configurations and evaluated them under three different weather conditions. Their findings proved that integrating the M-cycle with solar desiccant cooling systems showed better cooling performance than that hybrid with conventional evaporative coolers. The results also showed that the configuration with two M-cycle coolers in moderate and humid conditions reached the highest COP, 0.728 on average. Harrouz et al. [21] explored two desiccant-assisted evaporative cooling systems for the poultry industry in hot and humid climates. It was reported that the system using the M-cycle could maintain indoor thermal comfort and air quality with an operation cost that was 35% less than the system with a direct evaporative cooler (DEC). Lai et al. [22] numerically studied the influence of the recirculation air ratio on the performance of a solar-powered solid desiccant M-cycle system. The simulation

results highlighted that the product air humidity ratio and temperature could be lowered by 41.9% and 23.1%, respectively, as the return air ratio varied from 0% to 60%.

Previous studies have indicated that the M-cycle cooler is a vital option for sustainable cooling. The integration of a solid dehumidification process, which removes the moisture from the inlet air, can further extend the applicability of this technology in humid regions. However, these systems consume a large amount of water, which might add water scarcity for remote communities. On the other hand, desalinating seawater or brine water offers a possible way to overcome water scarcity. Among the existing desalination technologies, the humidification–dehumidification (HDH) desalination method showed some advantages, including a simpler structure, lower capital and maintenance costs, and compatibility with low-grade heat energy [23]. These features make it suitable for providing freshwater to residents in remote areas [24]. Therefore, hybridising the M-cycle cooling with HDH desalination for co-producing a cooling load and water has received significant research interest in these years.

Efforts have been made to harness the humid and warm waste air stream from the wet channel of the M-cycle cooler, which is typically released into the environment, to boost the efficiency of the HDH unit. Kabeel et al. [25] performed an experimental analysis on a new hybrid system consisting of an HDH desalination unit and an IEC cooler, powered by solar thermal energy. The results suggested that the developed system performed well in remote areas of Egypt and could produce more than 400 W of cooling load and 38 L of freshwater daily. Similarly, Chen et al. [26] combined an IEC with an HDH desalination unit in which the purged air from the IEC is used as the inlet air of the HDH to enhance freshwater productivity, and they compared the proposed system with other HDH cycles. Their findings revealed that the proposed system had better performance than the other configurations, with the water production rate and gain–output ratio (GOR) ranging from 25–125 L/h and 1.6–2.5, respectively. Abdelgaied et al. [27] conducted an experimental test that utilised a latent heat energy storage system to improve the performance of a hybrid IEC cooler and HDH system. The results showed that the studied hybrid system produced 14.6% more water than the original system, up to 241.7 L/day. On the other hand, the operation of a desiccant unit also produces hot and humid exhaust air during the regeneration process. Therefore, attempts have been made to reuse the desiccant exhaust air. Kabeel et al. [28] numerically examined a hybrid desiccant cooling system and an HDH desalination system. They concluded that the proposed system was feasible in hot and humid areas. Wang et al. [24] performed a numerical assessment of an innovative solid desiccant-assisted cooling system combined with an HDH desalination unit. In their developed system, the waste air from the regeneration process of the desiccant wheel was recycled as the inlet air of HDH. The authors reported that the developed system achieved the best performance when the air mass flow rate was 0.78 kg/s, resulting in the highest water production rate of 4.9 L/h.

In sum, it can be seen that the inclusion of a solid dehumidification unit significantly enhances the performance of the M-cycle, making evaporative cooling technology more practical in humid regions. Additionally, implementing HDH desalination technology is a practical approach to satisfying potable water needs. However, research on the combination of solid desiccant evaporative cooling systems and HDH desalination units is still insufficient. Recently, Lai et al. [29] investigated a new hybrid arrangement of a solid desiccant-assisted M-cycle cooling system combined with an HDH desalination unit that simultaneously utilised the two humid waste air streams from the M-cycle's wet channels and the desiccant wheel for water production. However, the influence of the operation strategy, comprising ventilation, recirculation, and half-recirculation modes, on the system's cooling and water production performance was not reported. To address this research gap, a numerical model was developed using TRNSYS software to explore the performance of a hybrid system that contains a solid desiccant-assisted M-cycle system and an HDH desalination unit under different operating modes. A comparative analysis was undertaken to assess the performance differentials of the developed system among its ventilation, recir-

culation, and half-recirculation modes, in the context of concurrent cooling and freshwater production. In this step, we also evaluated the impact of the operational parameters on the product air conditions (humidity and temperature), water consumption and production rates, cooling capacity, and COP for all three modes.

2. System Description

In this study, a co-producing cooling and water system was numerically investigated under ventilation, recirculation, and half-recirculation modes. The studied system is based on solid desiccant/evaporative cooling and HDH desalination technologies, as reported in our previous study [29]. A detailed explanation of the system's working principle for each operation mode is presented in the following sections.

2.1. Ventilation Mode

Figure 1 presents the schematic diagram of the proposed system (SDM-HDH) in ventilation mode and its working process on a psychrometric chart. There are two primary cycles in the SDM-HDH—the SDM cooling cycle and the HDH desalination cycle. The process of dehumidifying and cooling ambient air in the described system involves several steps. First, a desiccant wheel (1–2) is utilised to dehumidify the ambient air. The resulting dry, hot air is then cooled by flowing over a sensible heat wheel (2–3). The supply air is further cooled by the M-cycle cooler (3–4) before being distributed to the room for thermal comfort. To maintain the efficiency of the dehumidification process, a regeneration process is implemented. This involves mixing indoor and ambient air to provide a sufficient flow rate for the regeneration air, which flows over a heat wheel and exchanges heat with the hot supply air (5–6). The solar heater and auxiliary heater (6–7) further increase the temperature of the air stream to the required level for regeneration. The heated air stream then passes through the desiccant wheel (7–8) and removes the absorbed water. In the HDH desalination cycle, the inlet air (10) consists of the moist waste air from the rotary desiccant wheel (8) and the M-cycle cooler (9). This mixed air is sent to the humidifier, where it is further humidified and heated by the heated brine (10–11). The humid and hot airflow is then chilled and condensed in the dehumidifier by coming into contact with cold feed brine. The feed brine is pre-heated and then heated up to the required temperature level through solar and auxiliary heaters before being sprayed into the humidifier to complete the cycle.

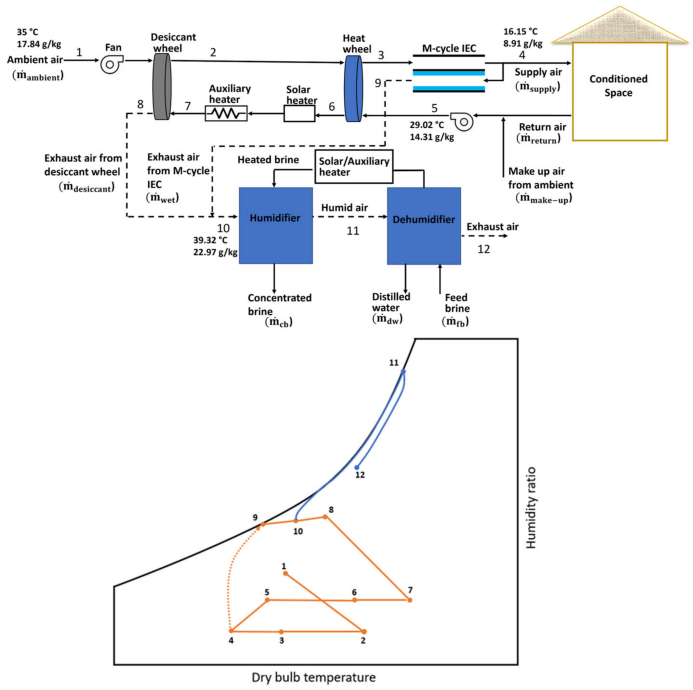

Figure 1. Schematic and psychrometric diagram of SDM-HDH in ventilation mode.

2.2. Recirculation and Half-Recirculation Mode

Figure 2 presents the operation of the SDM-HDH in recirculation mode and its process on a psychrometric diagram. In this mode, the return air from the conditioned space (6) is mixed with the ambient air (1) prior to undergoing dehumidification. The mixed air stream is then dried by a desiccant wheel (2–3) and pre-cooled by a rotary heat wheel (3–4). Subsequently, the air stream is further cooled by an M-cycle cooler before sending to the indoor space. In the regeneration part, the regeneration air is sourced from the environment, while the air from the conditioned space is used as recirculation air. The regeneration process is similar to that in the ventilation mode, with the exception of the air source. In the HDH water generation cycle, the exhaust air from the M-cycle (11) is combined with the desiccant wheel exhaust (10) and sent to the HDH to complete the process (12–14). In half-recirculation mode, the system combines 50% of the return air from the conditioned space with ambient air to form the process air stream. The remaining indoor air is used for the desiccant wheel regeneration. Aside from these distinctions, the other processes are the same as in recirculation mode.

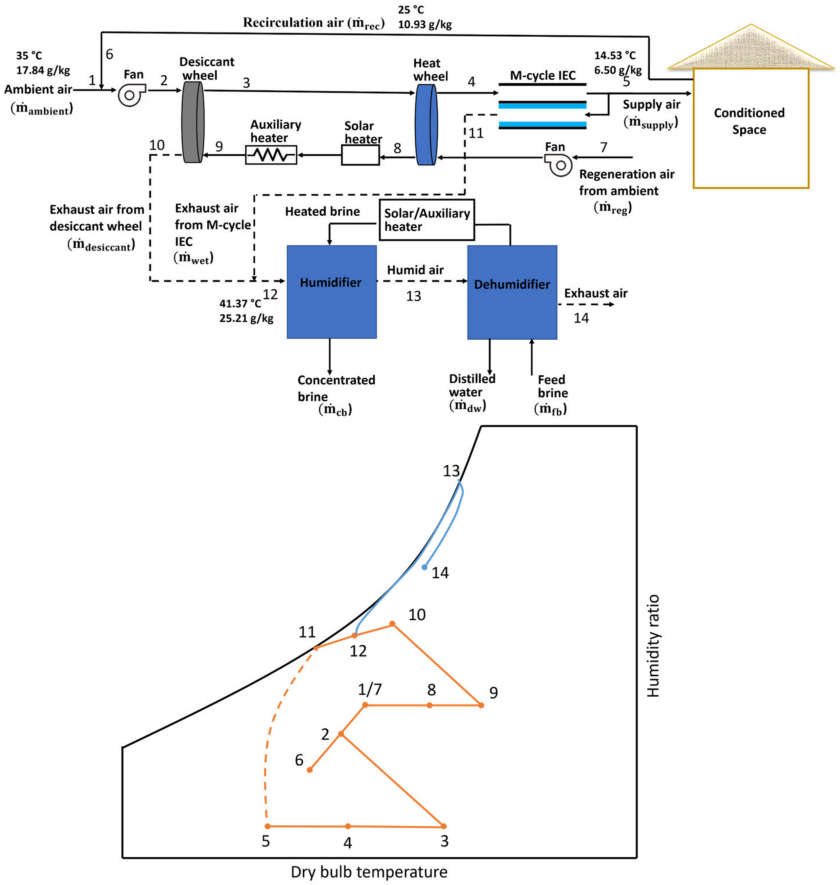

Figure 2. Schematic and psychrometric diagram of SDM-HDH in recirculation mode.

3. Mathematical Modelling

To compare the cooling performance and water productivity of the developed system in the ventilation, recirculation, and half-recirculation modes, commercial software TRNSYS 18 was utilised. TRNSYS is a widely used transient system modelling program that is particularly well-suited for air conditioning and renewable energy systems [30]. It features a flexible graphical interface that allows users to add and link system components easily, and its built-in library and supplementary library, TESS, includes more than 650 validated modules that can cover most of the commonly used components in this study, such as desiccant wheels, heat wheels, pumps, and fans [30,31]. Additionally, external software can be integrated with TRNSYS through the Calling External Programs function, allowing for the creation of new components. In this study, the M-cycle cooler and the HDH desalination unit were built using EES and connected to TRNSYS through the Calling External Programs function. The core components are listed in Table 1, and the detailed simulation of these components is explained and shown in the following sections.

Table 1. Descriptions of the main TRNSYS elements used in the simulation.

TRNSYS Component	Key Inputs	Description
Type 1716b–Desiccant wheel	Humidity mode: 1 ε_{F_1}: 0.05 ε_{F_2}: 0.95	High-performance rotary desiccant dehumidifier
Type 760–Heat wheel	Sensible effectiveness: 0.85 Humidity mode: 1	Air-to-air sensible rotary heat exchanger
Type 6–Electrical heater	Target temperature: 70 °C	Electrical heater, which heats the regeneration airflow to the target temperature
Type 112a–Fan blower	Airflow rate: 660 kg/h Efficiency: 0.9	Constant flow rate fan blower
Type 66–M-cycle IEC	Working/intake air ratio: 0.4 Height (Channel): 5 mm Height: 0.48 m Width: 0.28 m Length: 0.9 m	M-cycle-based indirect evaporative cooler
Type 66–HDH unit	ε_{hum}: 0.8 ε_{deh}: 0.8	HDH desalination unit
Type 65–Online plotter	–	Present the user-selected outputs

3.1. Rotary Desiccant Wheel

The rotary desiccant wheel plays a crucial role in the dehumidification process of the entire system. In this study, silica gel was chosen as the adsorbent material due to its low cost and good adsorption performance [32,33]. To predict the performance of the desiccant wheel, TRNSYS 18 used component Type 1716b, which is based on modelling equations developed by Jurinak [33]. These equations are derived from the potential functions F_1 and F_2, as shown in Equations (1) and (2).

$$F_1 = \frac{-2865}{T^{1.49}} + 4.34\omega^{0.8644} \quad (1)$$

$$F_2 = \frac{T^{1.49}}{6360} - 1.127\omega^{0.07969} \quad (2)$$

where T represents the airflow temperature, and ω represents the airflow humidity.

3.2. Rotary Heat Wheel

The heat wheel functions as a rotary heat exchanger, enabling sensible heat exchange between two air flows. It is available in TRNSYS as Type 760, and a constant effectiveness minimum capacitance model was used to set up the numerical models. The minimum capacitance is shown in Equation (3).

$$C_{min} = MIN\left(\dot{m}_1 c_{p1}, \dot{m}_2 c_{p2}\right) \quad (3)$$

where $\dot{m}_1$ and $\dot{m}_2$ are the mass flow rates of each airflow, c_{p1} and c_{p2} are the values of the specific heat of each working airflow. Then, the maximum sensible heat that can be transferred between air streams can be determined based on the minimum capacitance:

$$\dot{Q}_{sens} = \varepsilon_{sens} C_{min} |T_{1,\,in} - T_{2,\,in}| \quad (4)$$

where $\dot{Q}_{sens}$ is the maximum possible heat transfer rate between the two air flows inside the heat wheel, and ε_{sens} denotes the effectiveness of the rotary heat wheel.

3.3. M-Cycle Cooler

The M-cycle cooler is another crucial system component that produces a sensible cooling load. Since this component could not be found in the TRNSYS library, a mathematical model was created by considering the mass and heat balance equations inside the M-cycle cooler through the use of external software, EES. To integrate this model with TRNSYS, Type 66 was utilised in the TRNSYS interface to call the external program. The following assumptions were made in the derivation of the model:

- There is no heat loss to the surroundings;
- The wet channel's surface is completely wetted;
- The fluid properties within each control volume are uniform;
- The fluid flow is assumed to be incompressible;
- There is no temperature difference between the wet and dry channel surfaces.

In the dry channel of the M-cycle, the product air transfers sensible heat to the adjacent wet channel through the channel wall and a thin water film. The energy balance of a control volume in the dry channel can be described as follows:

$$\dot{m}_{dry} c_{p,\,dry} dT_{dry} = h_{c,dry}\left(T_{dry} - T_{wf}\right) dA \quad (5)$$

where $c_{p,\,dry}$ denotes the dry channel air's specific heat, $h_{c,dry}$ represents the heat transfer coefficient of the air inside the dry channel, T_{dry} denotes the air temperature inside the dry channel, and T_{wf} is the water film temperature in the wet channel.

Heat transfer occurs in the dry channels as the sensible heat is transferred to the adjacent wet channel, causing the water to evaporate and carry away the heat. Therefore, both mass and heat transfer must be considered inside the wet channel.

$$\dot{m}_{wet} c_{p,\,wet} dT_{wet} = h_{c,wet}(T_{wf} - T_{wet}) dA + L h_m(\omega_{wf} - \omega_{wet}) dA \quad (6)$$

$$\dot{m}_{wet} d\omega_{wet} = h_m(\omega_{wf} - \omega_{wet}) dA \quad (7)$$

where $c_{p,\,wet}$ means the wet channel air's specific heat, $h_{c,wet}$ represents the coefficient of the heat transfer of the moist air along the wet channel, L means the latent enthalpy of the vaporisation of water, h_m denotes the convective mass transfer coefficient, and ω_{wet} is the moist air humidity along the wet channel.

3.4. HDH Desalination Unit

The HDH desalination unit generates freshwater for the system. It is modelled using EES and connected to TRNSYS through Type 66, similar to the M-cycle model. The performance of the HDH unit, including the humidifier and dehumidifier, is predicted using the heat and mass balance equations within the unit. The assumptions and modelling equations used in this process are presented below [26,34–36]:

- Fluid properties are uniform in each part of the unit;
- The heat and mass transfer between the HDH and the ambient air are assumed to be minimal;
- The effectiveness of the HDH unit is assumed to be a constant value;
- Upon exiting the humidifier and dehumidifier, the air is assumed to be fully saturated.

$$\dot{m}_{fb} - \dot{m}_{10}(\omega_{11} - \omega_{10}) = \dot{m}_{cb} \quad (8)$$

$$\dot{m}_{fb} h_{hb,in} - \dot{m}_{cb} h_{cb} = \dot{m}_{10}(h_{11} - h_{10}) \quad (9)$$

$$\varepsilon_{hum} = \max\left\{\frac{h_{hb,in} - h_{cb}}{h_{hb,in} - h_{cb,idea}}, \frac{h_{11} - h_{10}}{h_{11,idea} - h_{10}}\right\} \quad (10)$$

where $\dot{m}_{fb}$ is the cold feed brine flowrate, $\dot{m}_{cb}$ is the concentrated brine flowrate, ε_{hum} is the humidifier's effectiveness, and $h_{hb,in}$ and h_{cb} represent the enthalpy of the heated and concentrated brine, respectively.

The heat and mass balance equations for the humidifier are presented in Equations (8) and (9), respectively. Equation (10) indicates the effectiveness of the humidifier. Similarly, the heat and mass balance equations for the dehumidifier are expressed in Equations (11) to (13).

$$\dot{m}_{10}(\omega_{11} - \omega_{12}) = \dot{m}_{dw} \tag{11}$$

$$\dot{m}_{10}(h_{11} - h_{12}) - \dot{m}_{dw}h_{dw} = \dot{m}_{fb}\left(h_{fb,out} - h_{fb,in}\right) \tag{12}$$

$$\varepsilon_{deh} = \max\{\frac{h_{fb,out} - h_{fb,in}}{h_{fb,out,idea} - h_{fb,in}}, \frac{h_{11} - h_{10}}{h_{11} - h_{10,idea}}\} \tag{13}$$

where $\dot{m}_{dw}$ represents the flowrate of distilled water, h_{dw} is the freshwater enthalpy, and ε_{deh} is the dehumidifier's effectiveness.

4. Performance Index

The water productivity of the system plays a vital role in determining the overall performance of the system. The HDH unit produces distilled freshwater, while the M-cycle cooler consumes water to produce a cooling load. Consequently, the net freshwater production rate of the entire system can be expressed as follows:

$$\dot{m}_{sys} = \dot{m}_{dw} - \dot{m}_{M-cycle} \tag{14}$$

where $\dot{m}_{sys}$ represents the net freshwater production rate, and $\dot{m}_{M-cycle}$ is the water consumption rate of the M-cycle, which can be calculated based on the humidity variation between the outlet and inlet of the wet channel.

The cooling capacity ($\dot{Q}_{cool}$) generated by the SDM is another vital performance metric that can be determined as:

$$\dot{Q}_{cool} = \dot{m}_4(h_4 - h_1) \tag{15}$$

In a traditional HDH desalination system, the GOR value is used to assess the system's water generation performance, expressed as the ratio of latent heat of generated water to the thermal energy input to the system, as shown in Equation (16). As the cooling performance was also considered in the system performance assessment, the overall system COP was adopted as the performance indicator, which can be expressed as the ratio of the water productivity and cooling load, which are the beneficial effects, to the thermal energy consumed for the regeneration process of the desiccant wheel and the heating load used in the HDH component, which is the overall consumed thermal energy.

$$GOR = \frac{\dot{m}_{dw}L}{\dot{Q}_{heat}} \tag{16}$$

$$\dot{Q}_{reg} = \dot{m}_5(h_7 - h_6) \tag{17}$$

$$\dot{Q}_{heat} = \dot{m}_{fb}\left(h_{fb,out} - h_{hb,in}\right) \tag{18}$$

$$COP = \frac{\dot{m}_{sys}L + \dot{Q}_{cool}}{\dot{Q}_{reg} + \dot{Q}_{heat}} \tag{19}$$

5. Model Verification

5.1. SDM Model Verification

As the M-cycle model was verified in our previously published work [22], and the other components in the SDM were available in the TRNSYS library, the SDM was validated by

comparing its dehumidification and cooling performance with the published experimental data from reference [18] under identical conditions, with inlet air temperatures ranging from 25 to 45 °C and the inlet air humidity levels varying from 12 to 18 g/kg. As shown in Figure 3, the maximum relative errors between the simulation and experimental results were 11.35% for the dehumidification performance and 7.56% for the supply air temperature. These results suggest that the developed model is effective in predicting the cooling and dehumidification performance of the system.

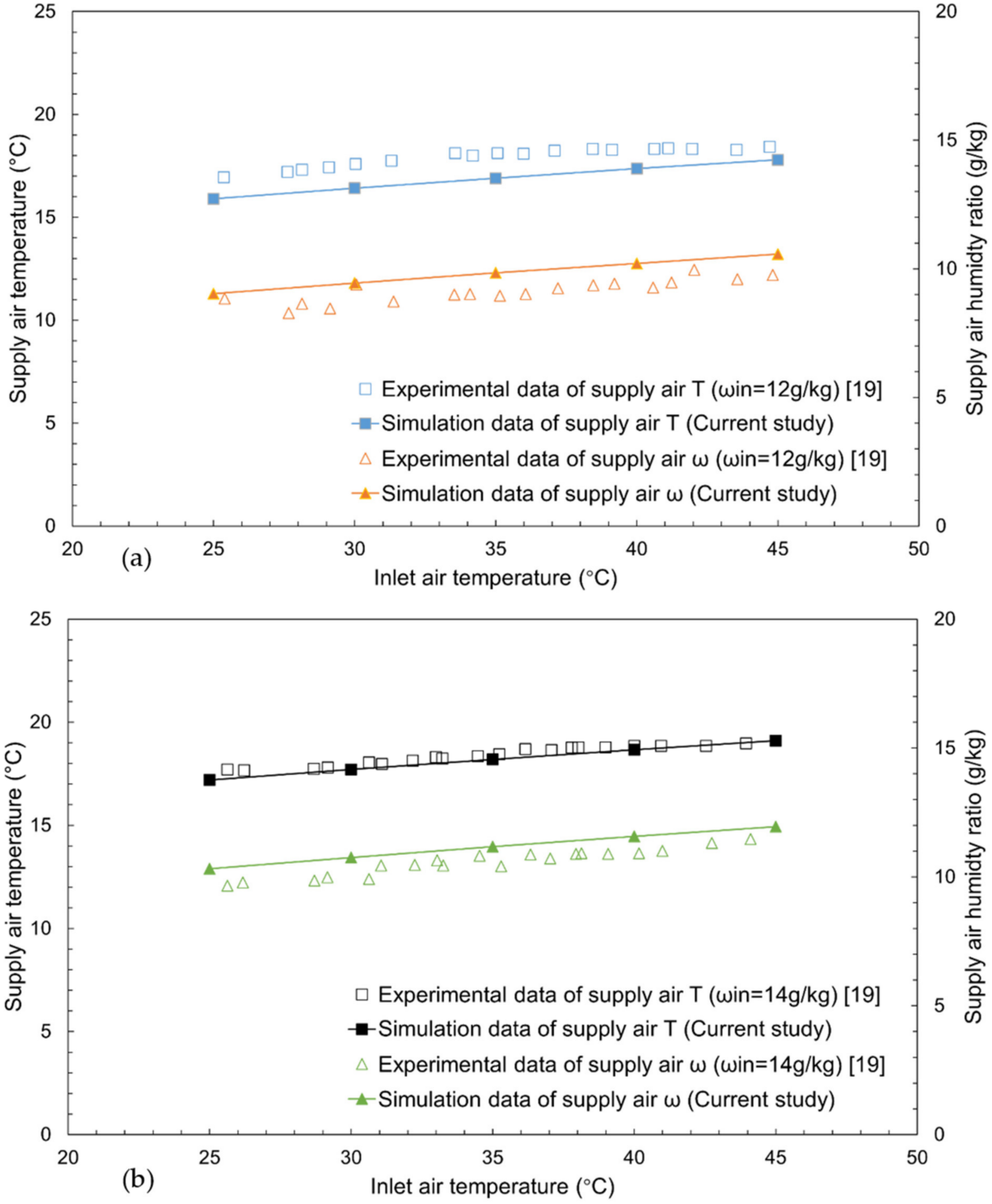

Figure 3. *Cont.*

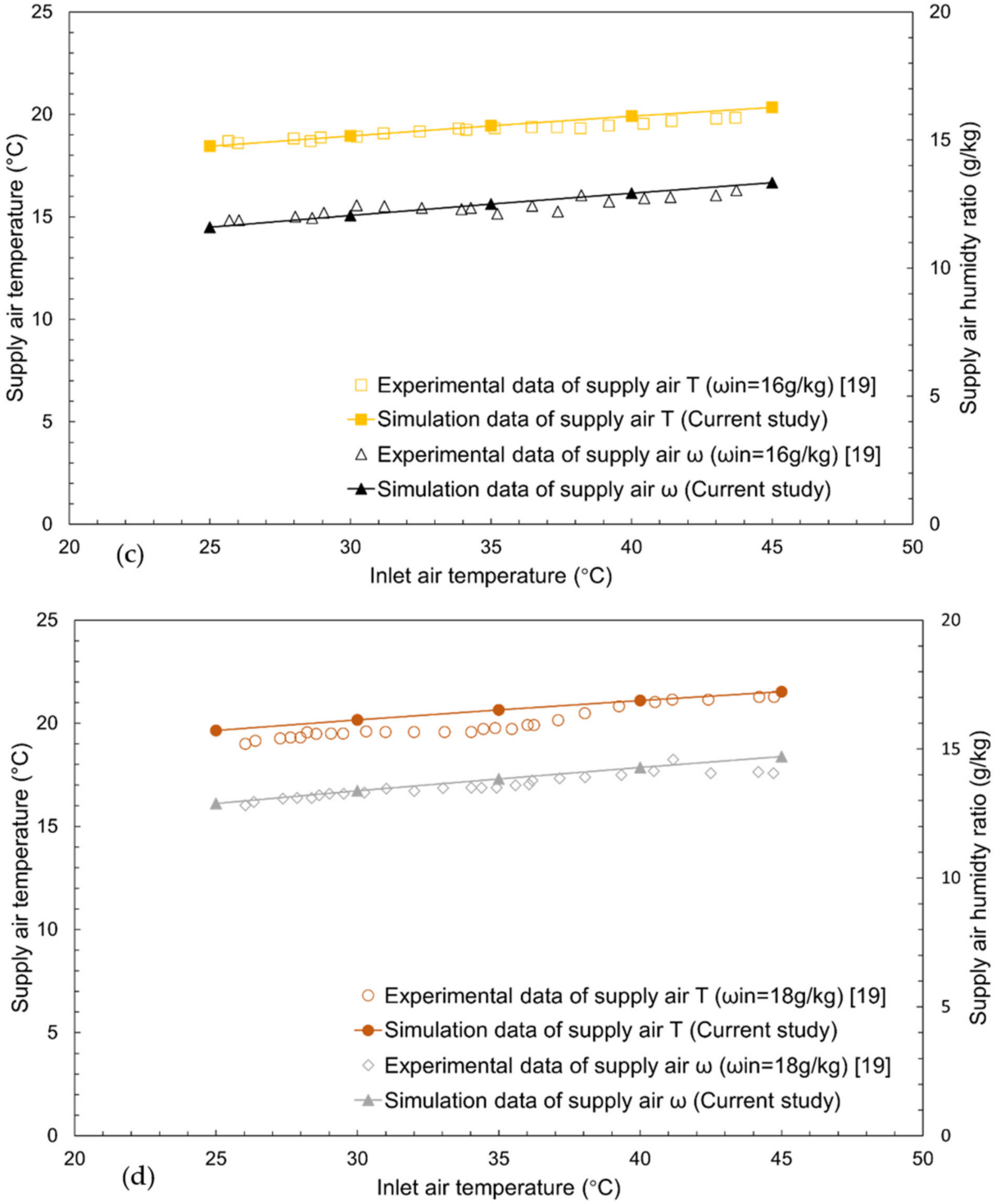

Figure 3. SDM model verification with experimental data from Ref. [18] at four different inlet air humidity levels: (**a**) ω_{in} = 12 g/kg; (**b**) ω_{in} = 14 g/kg; (**c**) ω_{in} = 16 g/kg; (**d**) ω_{in} = 18 g/kg.

5.2. HDH Model Verification

The model of HDH is verified by comparing the gain–output ratio (GOR) with the published data from reference [34]. Figure 4 shows the variation in the GOR between the current work and the published data at three different heating source levels, ranging from 60 °C to 80 °C, and various seawater-to-airflow rate ratios. It can be observed that the maximum discrepancy between these two studies is 4.7%, which demonstrates that the developed model can be used to predict HDH performance.

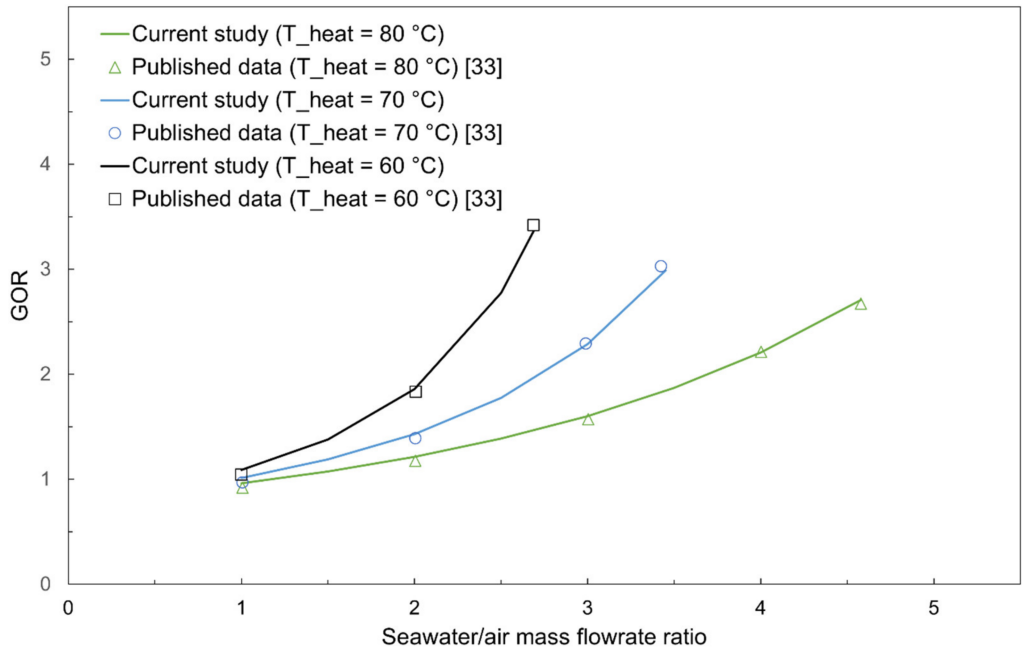

Figure 4. HDH model verification with published data [34].

6. Results and Discussions

In this study, the M-cycle cooling-based system combined with an HDH desalination unit was numerically evaluated and compared among the ventilation, recirculation and half-recirculation modes in terms of cooling performance, freshwater production rate, and overall system COP under different working conditions, using TRNSYS and EES. The proposed system integrates the SDM with the HDH unit, and the process air of the HDH component is a mixture of the exhaust of the desiccant wheel and M-cycle. The initial operating parameter settings are given in Table 2.

Table 2. Initial working conditions of the model.

Key Parameters	Value
Outdoor temperature	35 °C
Outdoor humidity ratio	50%
Process airflow rate	660 kg/h
Regeneration airflow rate	660 kg/h
Desiccant wheel regeneration temperature	70 °C
HDH unit heat source temperature	55 °C
Indoor temperature	25 °C
Indoor humidity ratio	55%

6.1. Cooling Performance Analysis

6.1.1. Comparison of Air Cooling Conditions under Various Ambient Temperatures

Figure 5 shows the comparison of product air states under different ambient air temperatures. It was observed that the SDM-HDH operating in the recirculation modes generated a supply of air that was cooler and drier than that in the ventilation mode. This was due to the return air emanating from the conditioned room, which tended to have a lower temperature and humidity than the ambient air. As presented in Figure 5a, the product air temperature of the system was comparable among the three operational modes, with a value of around 12 °C, while the temperature of the outdoor air was 30 °C. As the process air temperature increased from 30 to 45 °C, there was a corresponding increase in the product air temperature. Specifically, in the ventilation mode, the supply air temperature rose to 26.68 °C, while in the recirculation and half-recirculation modes, it increased to 20.85 °C and 24.10 °C. In Figure 5b, it can be seen that the humidity of

the product air surpassed the threshold of 20 g/kg, while the ambient air temperature surpassed 45 °C in the ventilation mode. Conversely, the recirculation mode produced a supply air stream that exhibited a humidity range of 4.457 to 12.72 g/kg, representing a dehumidification efficacy of up to 41.1% relative to the ventilation mode. These results indicate that the ventilation mode might not have been able to provide sufficient cooling at the high ambient air temperature, and recirculation was required to provide the cooling based on the ASHRAE cooling requirement.

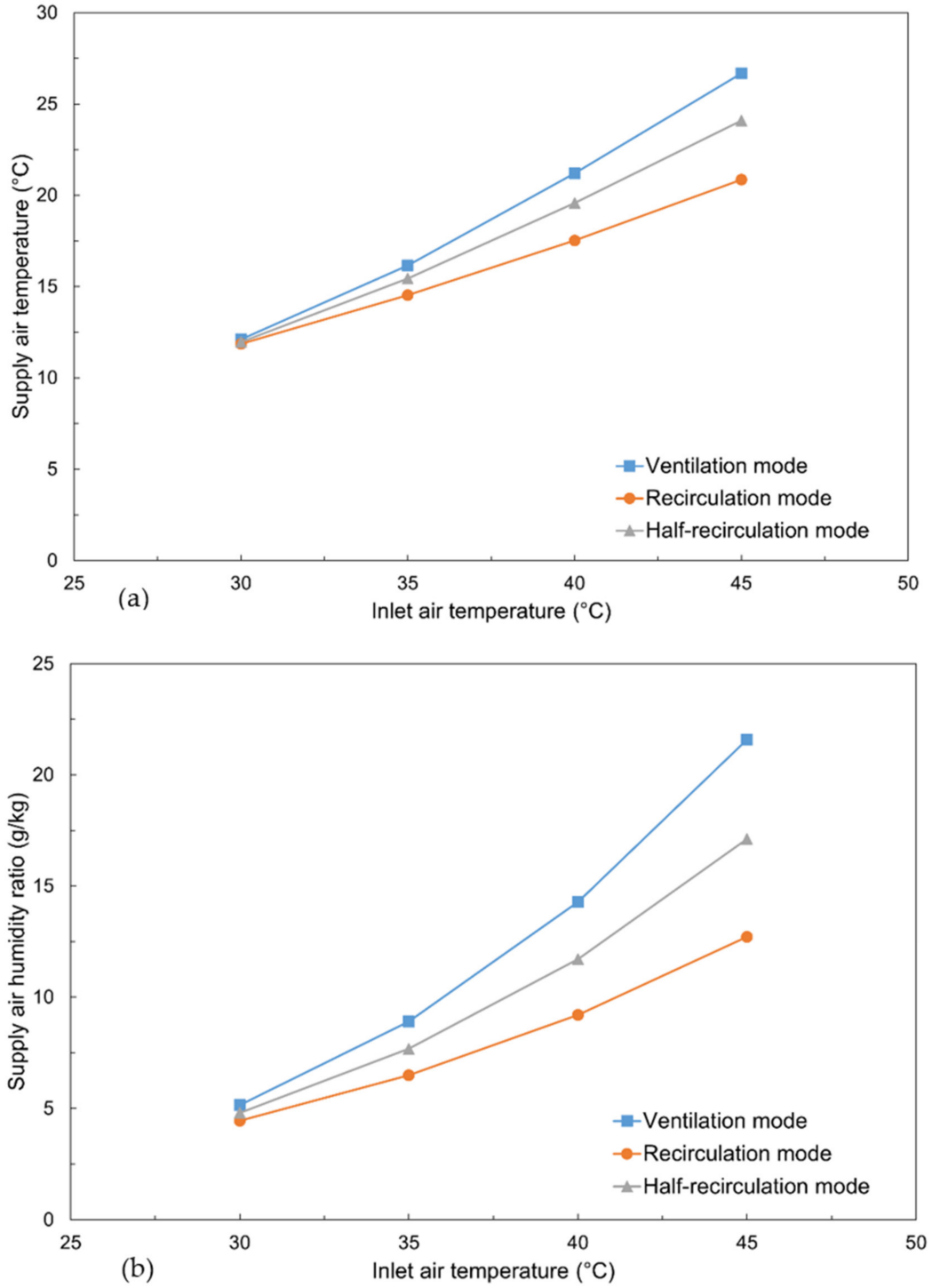

Figure 5. Effect of ambient temperature on supply air (**a**) temperature and (**b**) humidity.

6.1.2. Comparison of Product Air Conditions under Various Ambient Humidity Levels

The comparison of the product air states under different ambient air humidity levels is presented in Figure 6. It is shown that an increase in the ambient humidity ratio led to an increment in the product air temperature and humidity of all three operational modes. Figure 6a shows that, as the outdoor air humidity increased to 70%, the product air temperature of the system in the ventilation mode reached 20.99 °C. This can be attributed to the fact that the cooling efficiency of evaporative coolers is reduced in humid environments due to reduced evaporation. Similarly, the product air temperature of the system in the recirculation and half-recirculation modes also increased from 13.09 to 17.35 °C and 13.51 to 19.38 °C, respectively, as the outdoor humidity changed from 40 to 70%. As depicted in Figure 6b, the SDM system exhibited a robust latent cooling capability in all the operational modes, with the maximum humidity of the product air consistently maintained beneath 14.5 g/kg under conditions of an ambient humidity ratio of 70%. Furthermore, the supply air humidity in the system's recirculation mode was 22.3% to 30.3% lower than in the ventilation mode due to the inclusion of air from the conditioned room. These results further demonstrate that the recirculation mode is important to provide sufficient cooling for highly humid regions.

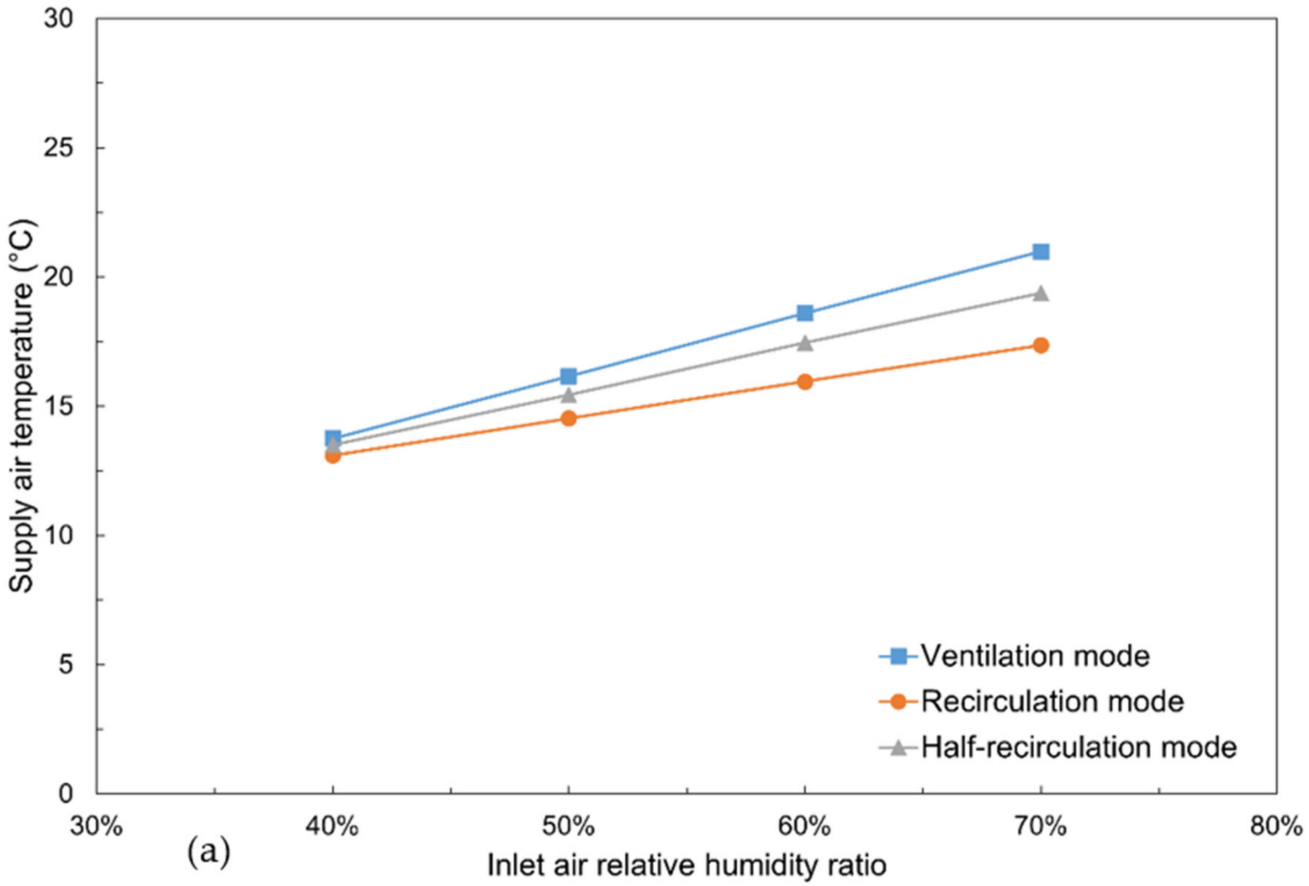

Figure 6. *Cont.*

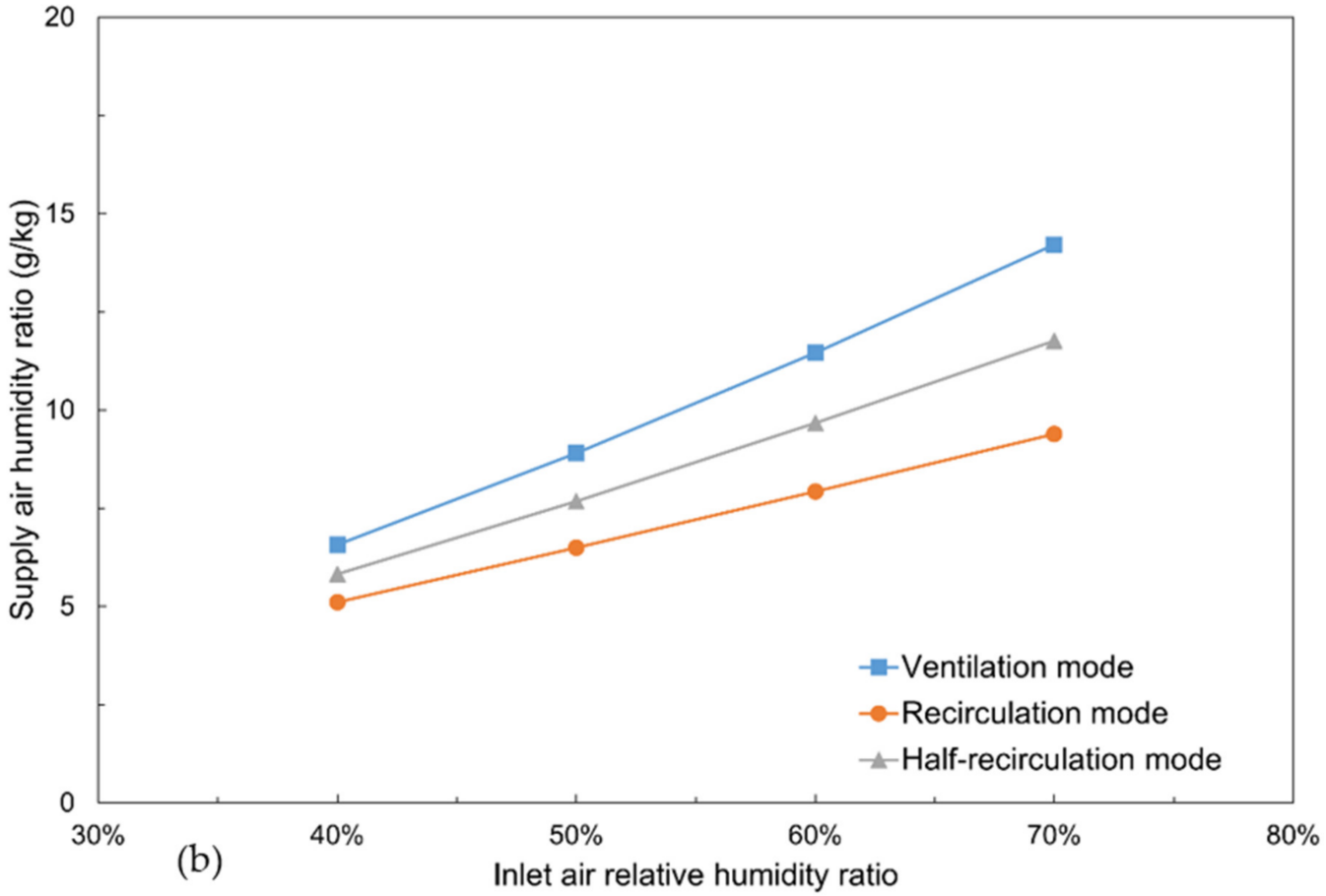

Figure 6. Effects of the ambient humidity on supply air (**a**) temperature and (**b**) humidity.

6.1.3. Comparison of Cooling Capacity under Various Ambient Conditions

In Figure 7, a comprehensive representation of the fluctuations in the cooling capacity of the proposed system, as it functions in three distinct modes, is presented in correlation to variations in the outdoor air conditions. The results reveal that the incorporation of the return air with the ambient air as the new supply air stream significantly enhanced the system's cooling performance. Figure 7a illustrates that the SDM in the ventilation mode generated 4.31 kW of cooling capacity at an ambient temperature of 30 °C, which slightly increased by 10.4% to reach 4.76 kW when the outdoor temperature reached 45 °C. However, when the system operated in the recirculation and half-recirculation modes, the cooling capacity exhibited a marked increase from 4.51 to 7.91 kW and 4.39 to 6.30 kW, respectively, within the same temperature range. The trends depicted in Figure 7b for various humidity levels demonstrate that the cooling capacity for all the modes increased as the environmental relative humidity ratio rose. As the environmental relative humidity increased from 40% to 70%, the cooling capacity for the ventilation, recirculation, and half-recirculation modes increased correspondingly, rising from 4.52 to 4.68 kW, 4.99 to 6.44 kW, and 4.38 to 5.55 kW, respectively. These results show that the system size can be reduced if the recirculation mode is used to provide cooling.

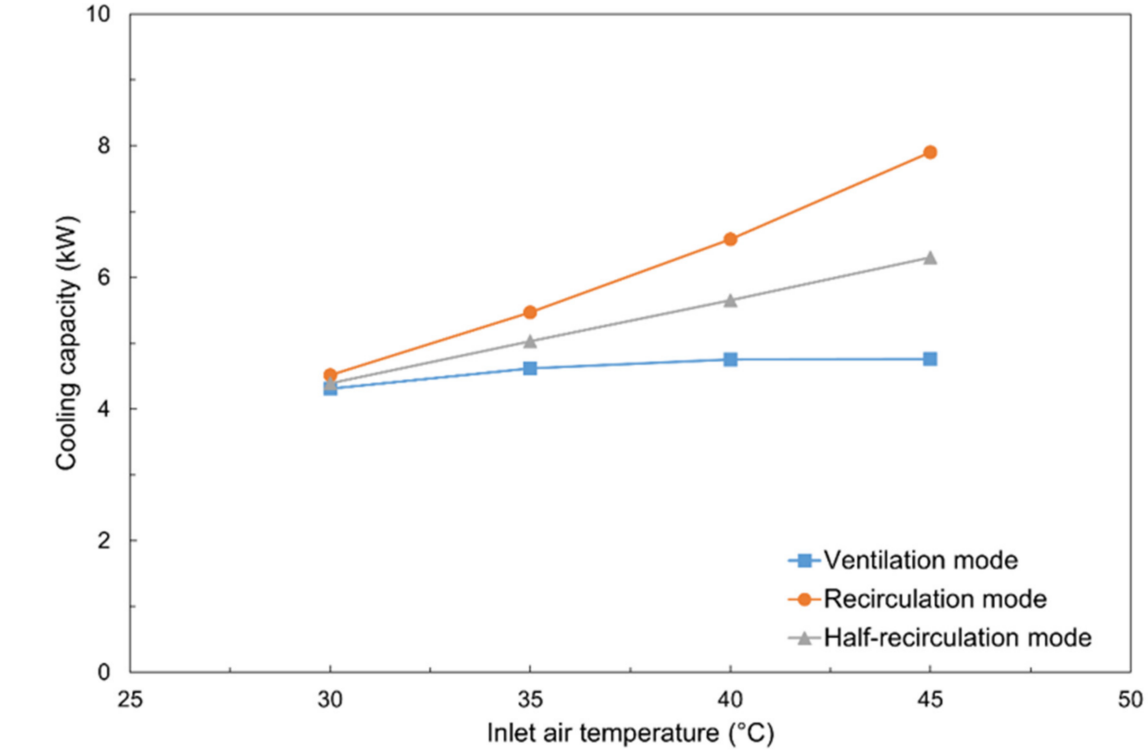

(a)

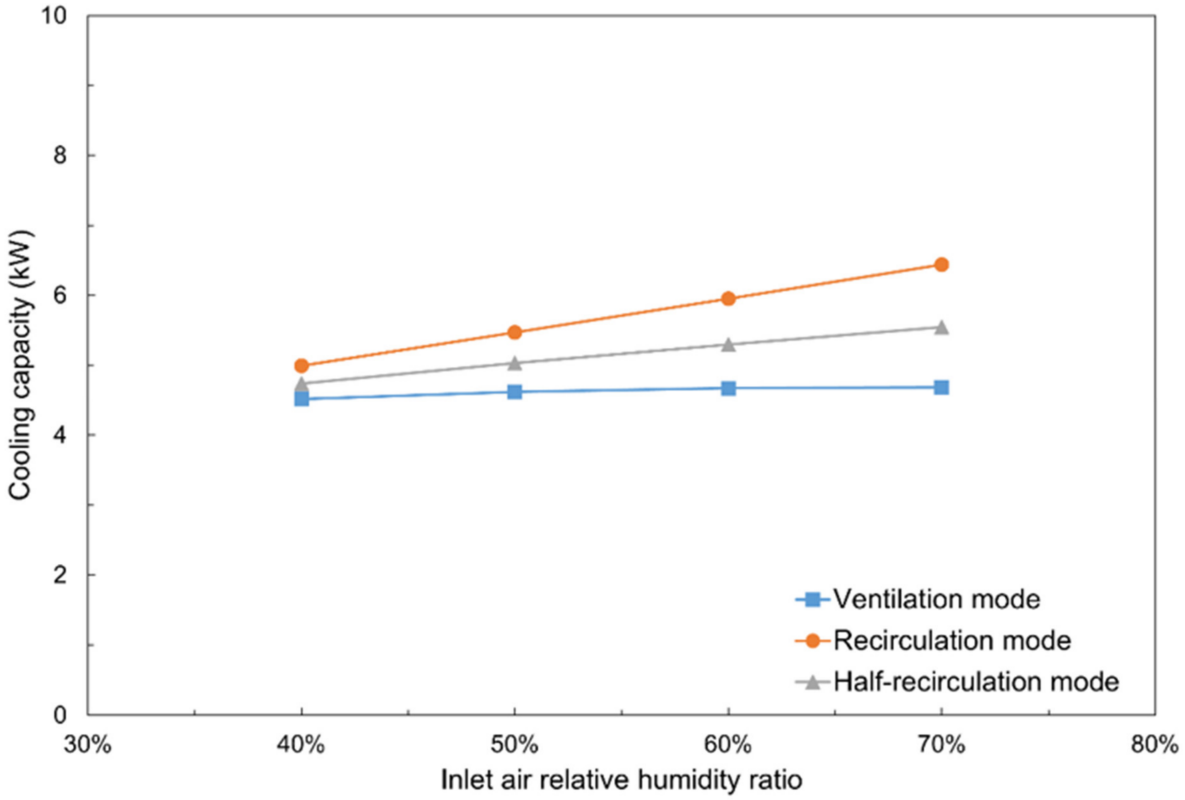

(b)

Figure 7. Effects of ambient air (**a**) temperature and (**b**) humidity on cooling capacity.

6.2. Water Production Analysis

6.2.1. Comparison of Water Usage Rate under Various Ambient Conditions

The SDM is a cooling system that relies on the water evaporation phenomenon to produce a cooling effect. In this case, the water consumption rate is also an important factor to consider in the operation and investigation of the system. Figure 8a illustrates that as the inlet air temperature increased, the water consumption rate in the ventilation mode decreased. This is because the desiccant wheel, which is a key component of the SDM, exhibited reduced dehumidification performance in hot and humid conditions, resulting in a reduced ability to evaporate water. In contrast, when the recirculation or the half-recirculation mode is implemented, the temperature and humidity ratio of the mixed air stream can be effectively reduced, which leads to a growth in the water usage rate. The highest water consumption rate was 5.52 kg/h when the system was operated in full recirculation mode at an ambient air temperature of 45 °C. The data depicted in Figure 8b demonstrate that as the humidity of the outdoor air increased, all the operational modes of the SDM exhibited a decrease in water consumption. Specifically, the freshwater usage rate dropped from 3.91 to 2.87 kg/h in the ventilation mode, from 4.99 to 4.25 kg/h in the recirculation mode, and from 4.47 to 3.58 kg/h in the half-recirculation mode. This reduction in water consumption can be attributed to the inhibitory effect of high humidity on the evaporation of water. It is clear that although the cooling capacity of the recirculation mode was higher, the water consumption rate was also much higher.

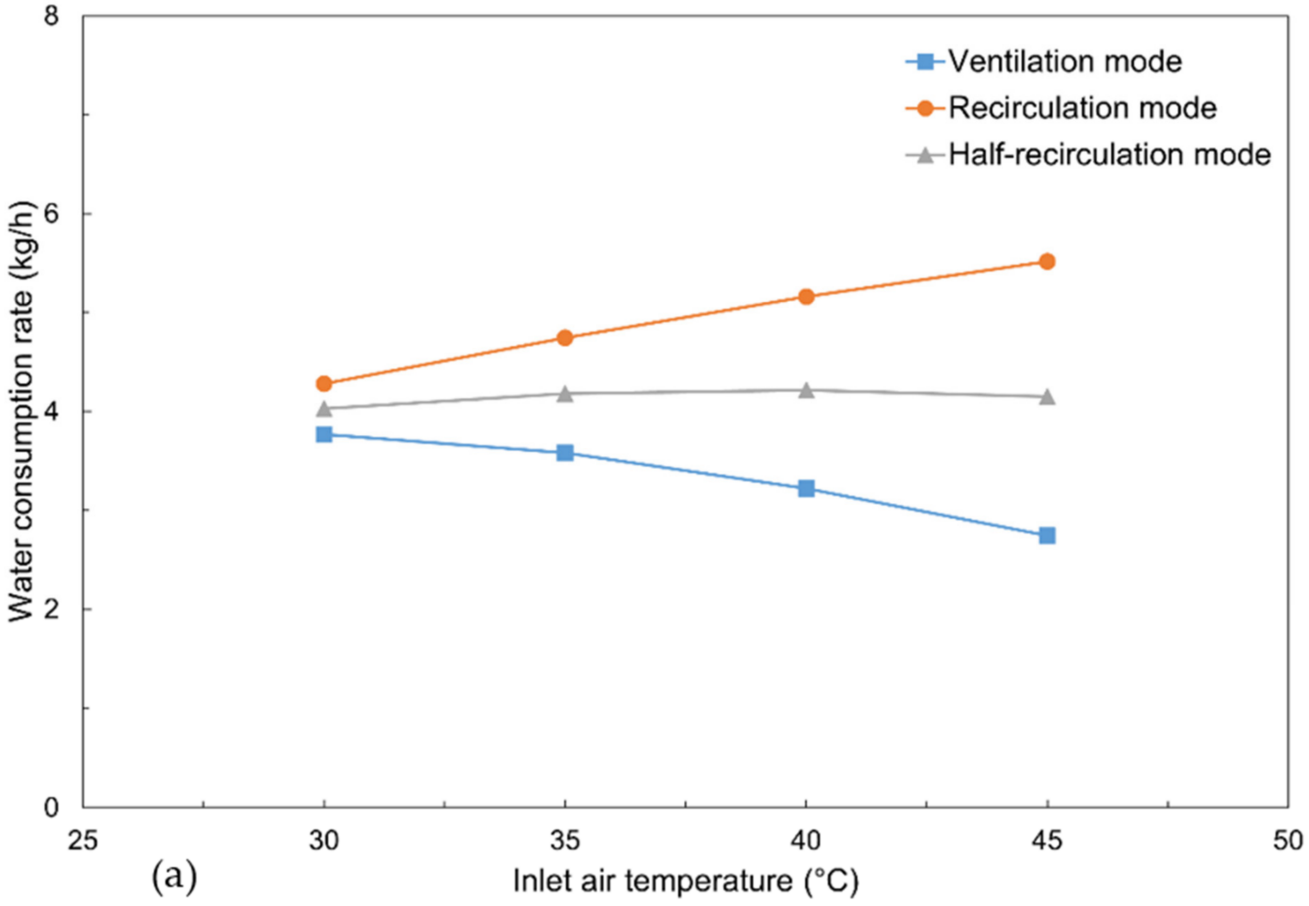

Figure 8. *Cont.*

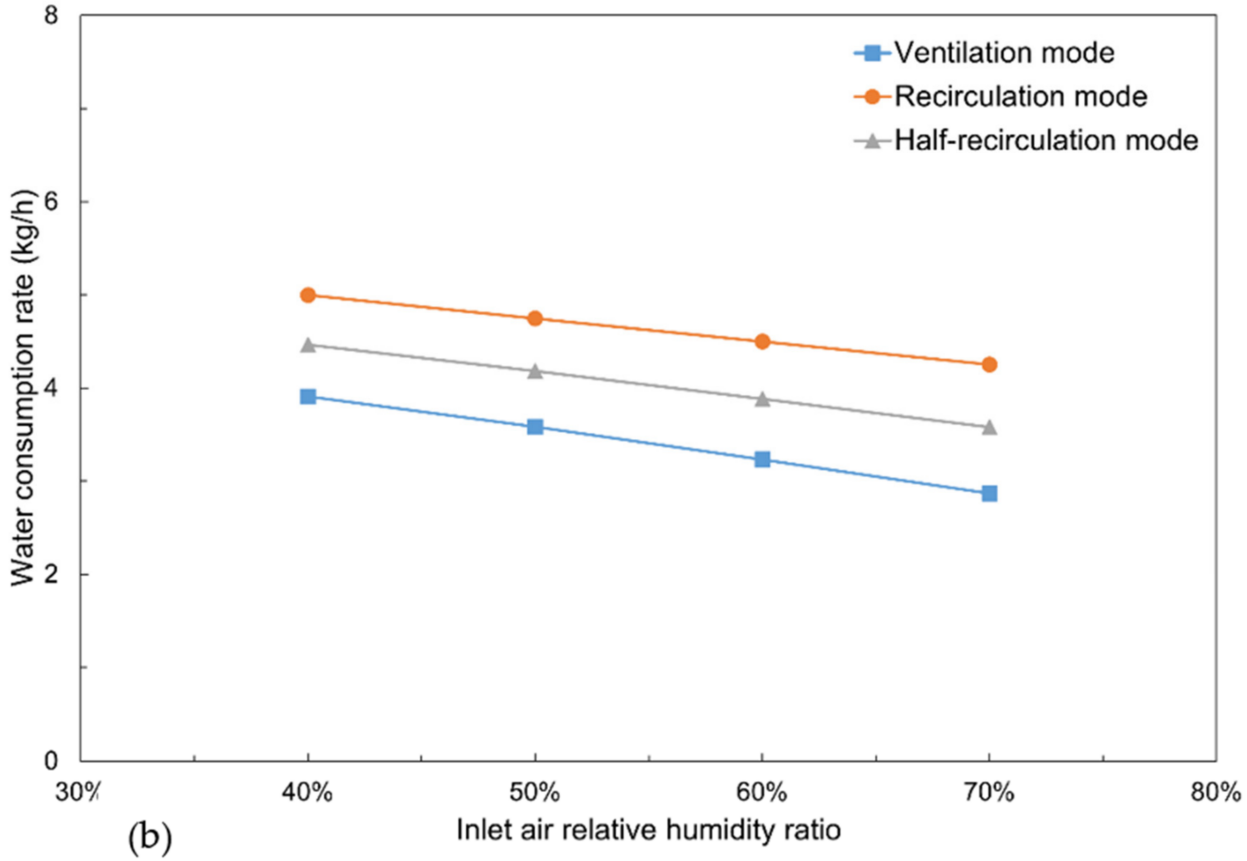

Figure 8. Effects of outdoor air (**a**) temperature and (**b**) humidity on water consumption rate.

6.2.2. Comparison of Water Production under Various Ambient Conditions

The comparative analysis depicted in Figure 9 reveals the impact of outdoor air conditions on the water productivity of the proposed system in different operational modes. The results indicate a relatively stable water productivity, with a minor increase observed as the ambient air became warmer and more humid. Figure 9a shows that the recirculation mode had the highest mean water productivity at 52.74 kg/h, followed by the half-recirculation mode with a mean of 52.43 kg/h, and the ventilation mode with the lowest mean of 52.14 kg/h. With the outdoor air temperature climbing to 45 °C, the water production rate for the recirculation mode slightly increased to 54.03 kg/h, representing a 1.12 kg/h increment compared to the ventilation mode. Figure 9b shows that the recirculation mode yielded a higher quantity of water at various humidity levels in comparison to the other two modes. For instance, when the outdoor humidity ratio reached 70%, the water production rates for the recirculation, half-recirculation, and ventilation modes were 53.06 kg/h, 52.68 kg/h, and 52.3 kg/h, respectively. These results show that the increase in water production was very small in the recirculation model. As presented in the water consumption section, the water consumption in the recirculation mode was much higher than in the ventilation mode. Therefore, it was important to evaluate the net water production in these three operation modes. As shown in Figure 9, upon considering the water consumption of each mode, it is apparent that the net water productivity of the ventilation mode surpassed that of the two recirculation modes at various environmental conditions, with a maximum difference of 1.65 kg/h at the outdoor air temperature of 45 °C. This is because the recirculation modes consumed more water compared to the ventilation mode under the same conditions, as demonstrated in Figure 8. These findings indicate that, although the two recirculation modes exhibited a slight advantage in the generation of freshwater over the ventilation mode, this advantage was offset by the higher water usage rate in the recirculation modes.

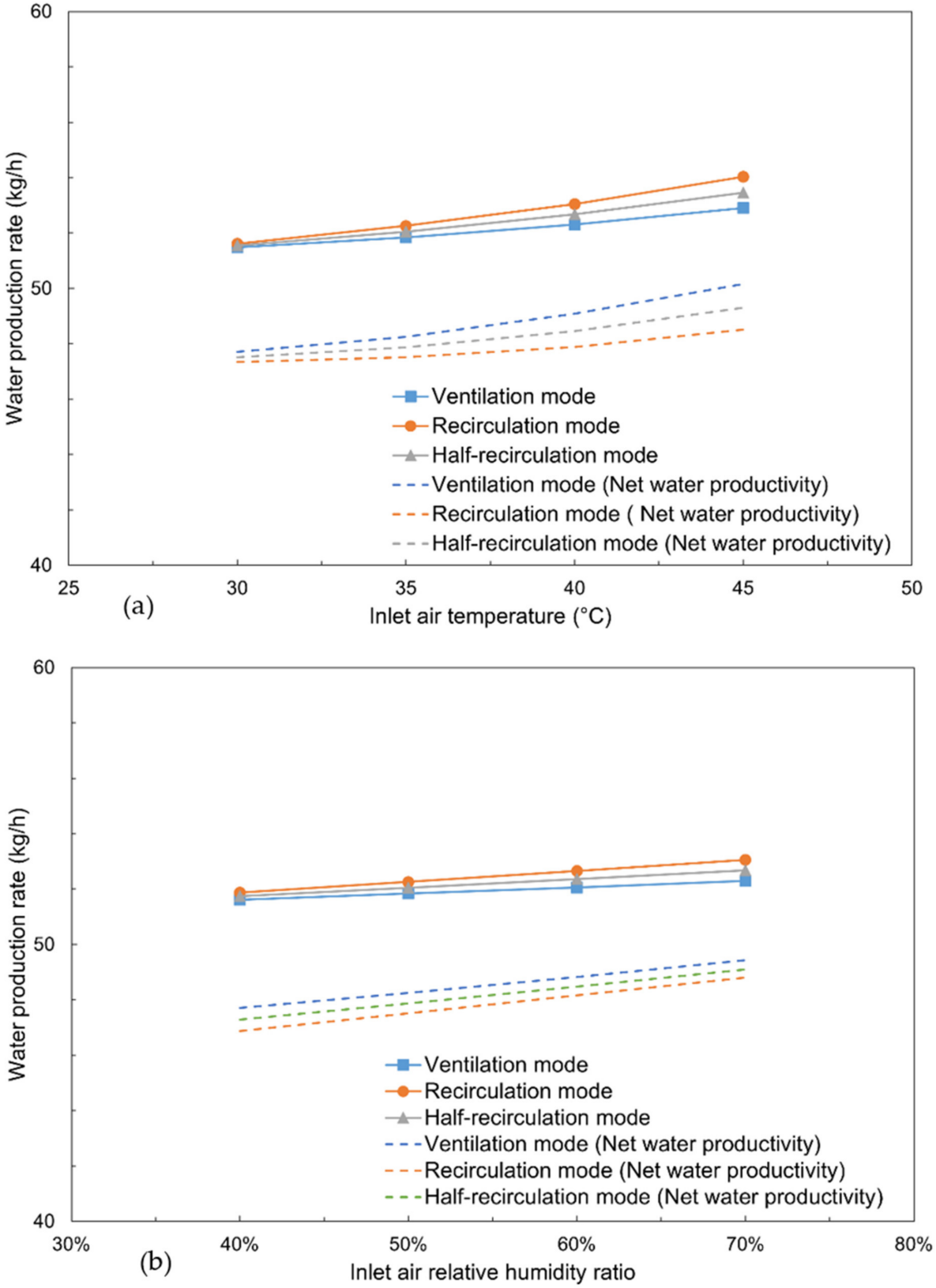

Figure 9. Effects of outdoor air (**a**) temperature and (**b**) humidity on water productivity.

6.2.3. Comparison of Water Production Rate at Various Heat Source Temperatures

The heat source temperature of the HDH unit plays a critical role in the system's water productivity, and it was therefore essential to consider its impact when assessing the overall

performance of the whole system. As demonstrated in Figure 10, an increase in the heat source temperature led to an augmented yield of distilled water. The water production rate for the ventilation, recirculation, and half-recirculation modes increased from 51.6 to 148.5 kg/h, 52.3 to 149.1 kg/h, and 52.05 to 148.9 kg/h, respectively, when the temperature of the heat source increased from 55 to 70 °C. This can be attributed to the fact that a higher heat source temperature enhanced the brine water evaporation potential within the humidifier of the HDH desalination unit. It is worth noting, however, that an increase in the heat source temperature also necessitated additional energy input for the purpose of heating the brine water. Additionally, it is evident that there was no discernible difference between the water production rate of the three operational modes at different heat source temperatures given that the inlet air conditions for the HDH unit were comparable at the selected working conditions (inlet air temperature of 35 °C and inlet air humidity ratio of 50%).

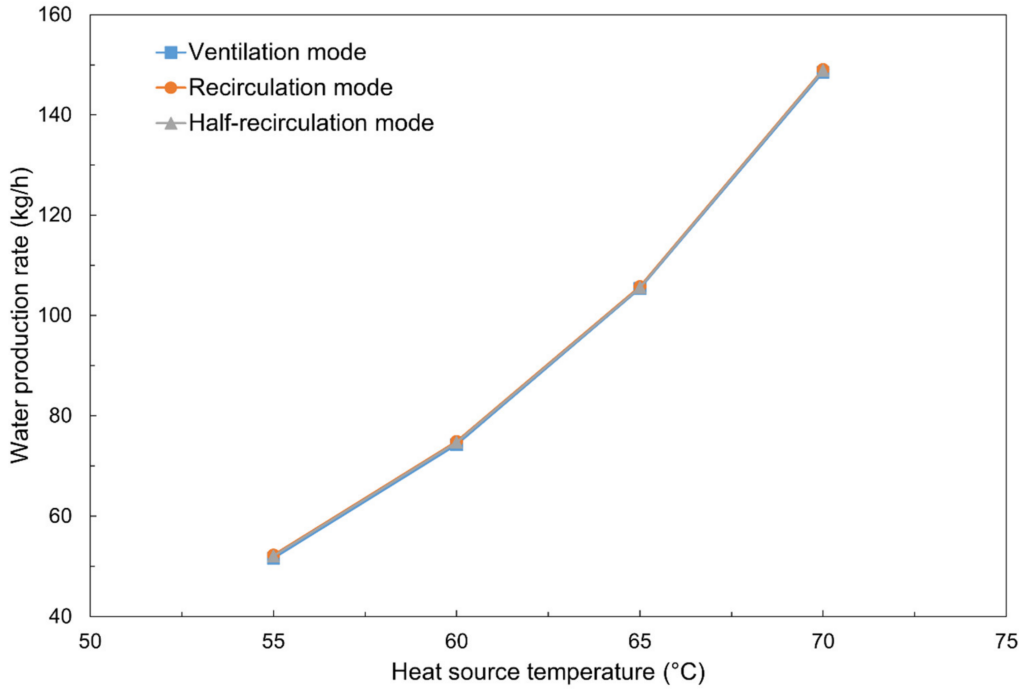

Figure 10. Effect of heat source temperature on water production rate.

6.3. Comparison of Overall System Performance Analysis (COP)

Figure 11 shows the change in the COP of the analysed system with respect to the various outdoor air conditions. It can be seen that the COP of all three modes increased slightly as the inlet air temperature and humidity ratio grew. This is because the cooling capacity and water productivity increased as the outdoor air became hot and humid for the three operational modes. It is imperative to observe that the COP for the recirculation and half-recirculation mode surpassed the ventilation mode when the inlet air temperature exceeded 35 °C and the inlet air humidity ratio was above 50%. However, the difference was very small. The maximum COP reached 0.44 at the inlet air temperature of 45 °C in the recirculation mode. This was mainly due to the more rapid growth in its cooling capacity in the recirculation modes in warmer and more humid conditions compared to the ventilation mode.

When considering the cooling capacity, water production, and system COP, the recirculation operating mode showed a slightly superior performance. This operating mode can provide the cooling requirement for users with a better system COP even at high ambient temperatures and relative humidity levels. Meanwhile, the net water production rate did not show much difference with the ventilation mode.

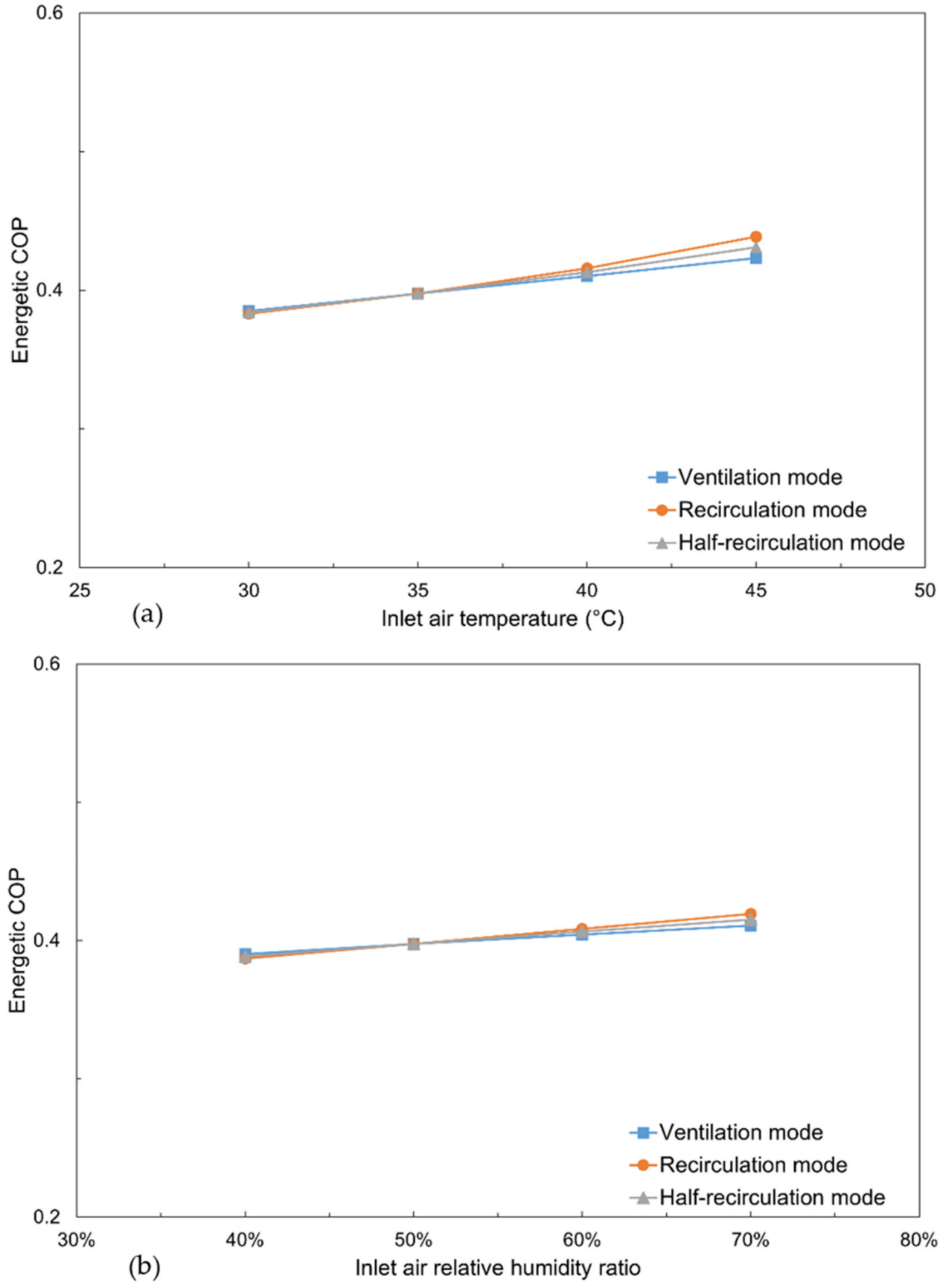

Figure 11. Effects of (**a**) ambient temperature and (**b**) humidity ratio on energetic COP.

7. Conclusions and Future Work

In the present study, a solid desiccant-based M-cycle cooling system (SDM) integrated with a humidification–dehumidification (HDH) unit was investigated under different working conditions through numerical simulation. To gain a deep understanding of the system, three operational modes were compared and assessed with respect to the cooling efficiency and water generation performance: ventilation, recirculation, and half-recirculation. The main findings of the study can be summarised as follows:

(1) The inclusion of the return air from a conditioned space in the recirculation and half-recirculation modes resulted in a superior cooling performance compared to the ventilation mode. In the recirculation mode, the system was able to generate up to 7.91 kW of cooling load and maintain the supply air temperature and humidity beneath 20.85 °C and 12.72 g/kg under various ambient conditions;

(2) The SDM-HDH system could effectively utilise the exhaust air from the solid desiccant M-cycle cooling system to generate water. All three operational modes exhibited an excellent water production rate, with average values of 52.74 kg/h, 52.43 kg/h, and 52.14 kg/h for the recirculation, half-recirculation, and ventilation modes, respectively, across a range of operating temperatures. In addition, adjusting the heat source temperature of the HDH component from 55 to 70 °C resulted in an increase in the water productivity of all the operational modes, with values ranging from 51.56 to 148.50 kg/h, 52.05 to 148.9 kg/h, and 52.26 to 149.1 kg/h for the ventilation, half-recirculation, and recirculation modes, respectively;

(3) It should be noted that the implementation of the recirculation mode resulted in the highest water consumption rate, with a value of 5.52 kg/h when the inlet air reached 45 °C, which partially offset the benefits of this mode. However, all three operating modes could provide net water production of up to 48 kg/h after considering the M-cycle water consumption;

(4) The overall energetic COP of all the operational modes increased slightly as the inlet air temperature and humidity ratio increased. The recirculation mode demonstrated a slightly better COP compared to the other two modes at ambient temperatures above 35 °C and the ambient humidity ratio above 50%. The maximum value of COP in the recirculation mode was 0.44 at the ambient temperature of 45 °C;

(5) In summary, this study has shown that the proposed system has good potential for producing cooling and water simultaneously. However, this study was based on the numerical method, and further experimental research and related economic analysis of the system should be conducted to understand the system better and evaluate the payback period. Moreover, future research could also focus on model improvements based on second-law analysis.

Author Contributions: Conceptualization, L.L. and X.W.; supervision, X.W., G.K. and E.H.; writing—L.L.; writing—review and editing, X.W., G.K. and E.H. All authors have read and agreed to the published version of the manuscript.

Funding: This research received no external funding.

Data Availability Statement: Data will be available on request.

Conflicts of Interest: The authors declare no conflict of interest.

Nomenclature

heat exchange area, m^2	A
coefficient of performance	COP
specific heat at constant pressure, kJ/kg·K	c_p
dew point temperature	DPT
potential functions 1 and 2 for desiccant wheel	F_1, F_2
enthalpy of moist air, J/kg	h
coefficient of heat transfer, W/m^2·K	h_c
humidification–dehumidification	HDH
mass transfer coefficient, m/s	h_m
latent enthalpy of vaporisation of water, J/kg	L
mass flow rate, kg/s	$\dot{m}$
heat transfer rate, kW	$\dot{Q}$
solid desiccant-based M-cycle cooling	SDM
temperature, °C	T
wet-bulb temperature	WBT
Greek Letters	
effectiveness	ε
humidity ratio of moist air, g/kg	ω
density, kg/m^3	ρ
Subscripts	
concentrated brine	cb
M-cycle's dry channels	dry
distilled water	dw
dehumidifier	deh
feed brine	fb
humidifier	hum
regeneration process	reg
sensible heat	sens
M-cycle's wet channels	wet
water film on the wet channel surface	wf

References

1. Mohammed, R.H.; Rezk, A.; Askalany, A.; Ali, E.; Zohir, A.; Sultan, M.; Ghazy, M.; Abdelkareem, M.; Olabi, A. Metal-organic frameworks in cooling and water desalination: Synthesis and application. *Renew. Sustain. Energy Rev.* **2021**, *149*, 111362. [CrossRef]
2. IEA. "The Future of Cooling," Paris. 2018. Available online: https://www.iea.org/reports/the-future-of-cooling (accessed on 1 September 2022).
3. Rocchetti, A.; Socci, L. Theoretical and numerical assessment of an enhanced Humidification-Dehumidification desalination system based on Indirect Evaporative cooling and Vapour Compression Refrigeration. *Appl. Therm. Eng.* **2022**, *208*, 118194. [CrossRef]
4. Abdelkareem, M.A.; El Haj Assad, M.; Sayed, E.; Soudan, B. Recent progress in the use of renewable energy sources to power water desalination plants. *Desalination* **2018**, *435*, 97–113. [CrossRef]
5. Sajjad, U.; Abbas, N.; Hamid, K.; Abbas, S.; Hussain, I.; Ammar, S.M.; Sultan, M.; Ali, H.M.; Hussain, M.; Rehman, T.U.; et al. A review of recent advances in indirect evaporative cooling technology. *Int. Commun. Heat Mass Transf.* **2021**, *122*, 105140. [CrossRef]
6. Shahzad, M.W.; Lin, J.; Xu, B.; Dala, L.; Chen, Q.; Burhan, M.; Sultan, M.; Worek, W.; Ng, K.C. A spatiotemporal indirect evaporative cooler enabled by transiently interceding water mist. *Energy* **2021**, *217*, 119352. [CrossRef]
7. Yang, H.; Shi, W.; Chen, Y.; Min, Y. Research development of indirect evaporative cooling technology: An updated review. *Renew. Sustain. Energy Rev.* **2021**, *145*, 111082. [CrossRef]
8. Chu, J.; Xu, W.; Fu, Y.; Huo, H. Experimental research on the cooling performance of a new regenerative dew point indirect evaporative cooler. *J. Build. Eng.* **2021**, *43*, 102921. [CrossRef]
9. Shahzad, M.W.; Burhan, M.; Ybyraiymkul, D.; Oh, S.; Ng, K.C. An improved indirect evaporative cooler experimental investigation. *Appl. Energy* **2019**, *256*, 113934. [CrossRef]

10. Mahmood, M.H.; Sultan, M.; Miyazaki, T.; Koyama, S.; Maisotsenko, V.S. Overview of the Maisotsenko cycle—A way towards dew point evaporative cooling. *Renew. Sustain. Energy Rev.* **2016**, *66*, 537–555. [CrossRef]
11. Baakeem, S.S.; Orfi, J.; Mohamad, A.; Bawazeer, S. The possibility of using a novel dew point air cooling system (M-Cycle) for A/C application in Arab Gulf Countries. *Build. Environ.* **2019**, *148*, 185–197. [CrossRef]
12. Lai, L.; Wang, X.; Kefayati, G.; Hu, E. Evaporative Cooling Integrated with Solid Desiccant Systems: A Review. *Energies* **2021**, *14*, 5982. [CrossRef]
13. Chaudhary, G.Q.; Ali, M.; Sheikh, N.A.; Gilani, S.I.U.H.; Khushnood, S. Integration of solar assisted solid desiccant cooling system with an efficient evaporative cooling technique for separate load handling. *Appl. Therm. Eng.* **2018**, *140*, 696–706. [CrossRef]
14. Goldsworthy, M.; White, S. Optimisation of a desiccant cooling system design with an indirect evaporative cooler. *Int. J. Refrig.* **2011**, *34*, 148–158. [CrossRef]
15. Gao, W.; Worek, W.; Konduru, V.; Adensin, K. Numerical study on performance of a desiccant cooling system with an indirect evaporative cooler. *Energy Build.* **2015**, *86*, 16–24. [CrossRef]
16. Gadalla, M.; Saghafifar, M. Performance assessment and transient optimisation of air precooling in multi-stage solid desiccant air conditioning systems. *Energy Convers. Manag.* **2016**, *119*, 187–202. [CrossRef]
17. Lin, J.; Wang, R.; Kumja, M.; Bui, T.; Chua, K.J. Modelling and experimental investigation of the cross-flow dew point evaporative cooler with and without dehumidification. *Appl. Therm. Eng.* **2017**, *121*, 1–13. [CrossRef]
18. Shahzad, M.K.; Chaudhary, G.Q.; Ali, M.; Sheikh, N.A.; Khalil, M.S.; Rashid, T.U. Experimental evaluation of a solid desiccant system integrated with cross flow Maisotsenko cycle evaporative cooler. *Appl. Therm. Eng.* **2018**, *128*, 1476–1487. [CrossRef]
19. Pandelidis, D.; Pacak, A.; Cichoń, A.; Drąg, P.; Worek, W.; Cetin, S. Numerical and experimental analysis of precooled desiccant system. *Appl. Therm. Eng.* **2020**, *181*, 115929. [CrossRef]
20. Delfani, S.; Karami, M. Transient simulation of solar desiccant/M-Cycle cooling systems in three different climatic conditions. *J. Build. Eng.* **2020**, *29*, 101152. [CrossRef]
21. Harrouz, J.P.; Katramiz, E.; Ghali, K.; Ouahrani, D.; Ghaddar, N. Comparative analysis of sustainable desiccant—Evaporative based ventilation systems for a typical Qatari poultry house. *Energy Convers. Manag.* **2021**, *245*, 114556. [CrossRef]
22. Lai, L.; Wang, X.; Kefayati, G.; Hu, E. Performance evaluation of a solar powered solid desiccant evaporative cooling system with different recirculation air ratios. *Energy Build.* **2022**, *270*, 112273. [CrossRef]
23. Xu, H.; Jiang, S.; Xie, M.; Jia, T.; Dai, Y.J. Technical improvements and perspectives on humidification-dehumidification desalination—A review. *Desalination* **2022**, *541*, 116029. [CrossRef]
24. Wang, N.; Wang, D.; Dong, J.; Wang, H.; Wang, R.; Shao, L.; Zhu, Y. Performance assessment of PCM-based solar energy assisted desiccant air conditioning system combined with a humidification-dehumidification desalination unit. *Desalination* **2020**, *496*, 114705. [CrossRef]
25. Kabeel, A.E.; Abdelgaied, M.; Feddaoui, M.B. Hybrid system of an indirect evaporative air cooler and HDH desalination system assisted by solar energy for remote areas. *Desalination* **2018**, *439*, 162–167. [CrossRef]
26. Chen, Q.; Burhan, M.; Shahzad, M.; Ybyraiymkul, D.; Akhtar, F.; Ng, K.C. Simultaneous production of cooling and freshwater by an integrated indirect evaporative cooling and humidification-dehumidification desalination cycle. *Energy Convers. Manag.* **2020**, *221*, 113169. [CrossRef]
27. Abdelgaied, M.; Kabeel, A.; Ezat, A.; Dawood, M.K.; Nabil, T. Performance improvement of the hybrid indirect evaporative type air cooler and HDH desalination system using shell and tube latent heat energy storage tank. *Process. Saf. Environ. Prot.* **2022**, *168*, 800–809. [CrossRef]
28. Kabeel, A.E.; Abdelgaied, M.; Zakaria, Y. Performance evaluation of a solar energy assisted hybrid desiccant air conditioner integrated with HDH desalination system. *Energy Convers. Manag.* **2017**, *150*, 382–391. [CrossRef]
29. Lai, L.; Wang, X.; Kefayati, G.; Hu, E. Analysis of a novel solid desiccant evaporative cooling system integrated with a humidification-dehumidification desalination unit. *Desalination* **2023**, *550*, 116394. [CrossRef]
30. Klein, S.A.; Beckman, W.A. *TRNSYS 18: A Transient System Simulation Program*; Solar Energy Laboratory, University of Wisconsin: Madison, WI, USA, 2017; Available online: http://sel.me.wisc.edu/trnsys (accessed on 1 September 2022).
31. Fong, K.F.; Lee, C.K. Solar desiccant cooling system for hot and humid region—A new perspective and investigation. *Solar Energy* **2020**, *195*, 677–684. [CrossRef]
32. El Loubani, M.; Ghaddar, N.; Ghali, K.; Itani, M. Hybrid cooling system integrating PCM-desiccant dehumidification and personal evaporative cooling for hot and humid climates. *J. Build. Eng.* **2020**, *33*, 101580. [CrossRef]
33. Zheng, X.; Ge, T.; Wang, R.Z. Recent progress on desiccant materials for solid desiccant cooling systems. *Energy* **2014**, *74*, 280–294. [CrossRef]
34. Narayan, G.P.; Sharqawy, M.; Lienhard, V.J.; Zubair, S.M. Thermodynamic analysis of humidification dehumidification desalination cycles. *Desalination Water Treat.* **2010**, *16*, 339–353. [CrossRef]

35. Sadeghi, M.; Yari, M.; Mahmoudi, S.; Jafari, M. Thermodynamic analysis and optimisation of a novel combined power and ejector refrigeration cycle—Desalination system. *Appl. Energy* **2017**, *208*, 239–251. [CrossRef]
36. Narayan, G.P.; McGovern, R.; Zubair, S.; Lienhard, J.H. High-temperature-steam-driven, varied-pressure, humidification-dehumidification system coupled with reverse osmosis for energy-efficient seawater desalination. *Energy* **2012**, *37*, 482–493. [CrossRef]